Experimental Measurement and Thermodynamic Modeling of Water Content in Methane and Ethane Systems

ARTICLE *in* INDUSTRIAL & ENGINEERING CHEMISTRY RESEARCH · SEPTEMBER 2004

Impact Factor: 2.59 · DOI: 10.1021/ie049843f

4 AUTHORS:

Amir H. Mohammadi

557 PUBLICATIONS **4,820** CITATIONS

SEE PROFILE

Antonin Chapoy

Heriot-Watt University

106 PUBLICATIONS **1,669** CITATIONS

SEE PROFILE

Dominique Richon

Aalto University

533 PUBLICATIONS **6,603** CITATIONS

SEE PROFILE

Bahman Tohidi

Heriot-Watt University

216 PUBLICATIONS **3,099** CITATIONS

SEE PROFILE

Experimental Measurement and Thermodynamic Modeling of Water Content in Methane and Ethane Systems

Amir H. Mohammadi,[†] Antonin Chapoy,[‡] Dominique Richon,[‡] and Bahman Tohidi*[,†]

Centre for Gas Hydrate Research, Institute of Petroleum Engineering, Heriot-Watt University, Edinburgh EH14 4AS, Scotland, U.K., and Centre d'Energétique, Ecole Nationale Supérieure des Mines de Paris, CENERG/TEP, 35 Rue Saint Honoré, 77305 Fontainebleau, France

In this article, we first report a summary of experimental methods used for measuring water content and water dew point of gaseous systems. After reviewing the available water content data in the literature, new experimental data and thermodynamic modeling on the amount of water in methane and ethane systems are reported. Equilibrium measurements are conducted at 282.98−313.12 K and 282.93−293.10 K and pressures up to 2.846 and 2.99 MPa, respectively. A static-analytic apparatus has been used in the experimental measurements, taking advantage of a pneumatic capillary sampler in combination with an exponential dilutor. The Valderrama modification of Patel−Teja equation of state with the nondensity dependent mixing rules are used for modeling the fluid phases with the previously reported binary interaction parameters. The hydrate phase is modeled by the solid solution theory of van der Waals and Platteeuw, using the previously reported Kihara potential parameters. The fugacity of ice is calculated by correcting the saturation fugacity of water at the same temperature by using the Poynting correction. The experimental data generated in this work were compared with predictions of the thermodynamic model as well as other predictive methods. The predictions were in good agreement with the experimental data, demonstrating the reliability of experimental techniques and thermodynamic modeling used in this work.

1. Introduction

Natural gases are generally saturated with water at reservoir conditions. During production, transportation, and processing, some of the dissolved water in the vapor phase may condense. The condensed water may contribute to gas hydrates and/or ice formation under specific temperature and pressure conditions. This phenomenon can arise during transportation in pipelines with large temperature gradients.

Forming a condensed water phase may lead to corrosion and/or two-phase flow problems. The formation of gas hydrates and/or ice could result in pipelines blockage and shutdown. To avoid these problems, accurate knowledge of water−hydrocarbon phase behavior is of great interest to the petroleum industry. On the other hand, estimating water content is crucial in the design and operation of natural gas facilities. However, most of experimental data on water content for hydrocarbons and non-hydrocarbon gases (e.g., nitrogen, carbon dioxide, and hydrogen sulfide) at low temperature conditions are scarce and often rather dispersed. It seems that achieving equilibrium at low temperature conditions, especially near and inside hydrate forming conditions, is a very slow process and requires a long time. At rather low temperatures and high pressures conditions, the water content of a gas is indeed very low. It is well-known that the determination of water traces in gases is one of the most difficult problems of trace analyses, and their accurate measurements require very specialized techniques.

To give a qualified estimate of the amount of water in the gas phase, predictive methods are required. General methods of calculation include the use of the following: (1) empirical or semiempirical equations and plots of water content versus pressure and temperature and corrections for the presence of acid gases such as hydrogen sulfide and carbon dioxide or heavy hydrocarbons and salts (e.g. Ideal model, Ideal model + Poynting correction, Bukacek correlation,[1] Sharma−Campbell method,[2] Robinson et al. chart,[3] Maddox et al. correlation,[4] Wichert−Wichert correlation,[5] McKetta−Wehe chart,[6] and Ning et al. correlation[7]) and (2) thermodynamic models which are based on equality of chemical potential of various components in different phases.

The aim of this work is to study phase equilibria in water−methane and water−ethane systems by generating new experimental data as well as extending a thermodynamic model to low-temperature conditions. For this purpose a review is made on popular methods for measuring water content/water dew point of gases. Then the water content data for natural gas main components are gathered from the literature. An apparatus based on a static-analytic method combined with a dilutor apparatus to calibrate the gas chromatograph (*GC*) detectors with water is used to measure the water content of methane and ethane.

A thermodynamic model based on the Valderrama modification of the Patel and Teja equation of state (*VPT−EoS*)[8] with the nondensity dependent (*NDD*) mixing rules[9] is used for predicting phase equilibrium. In this model, the fugacity of ice is calculated by correcting the saturation fugacity of water at the same temperature by an exponential factor (the Poynting correction). The hydrate phase is modeled by the solid

* To whom correspondence should be addressed. Tel.: +44 (0)131 451 3672. Fax: +44 (0)131 451 3127. E-mail: Bahman.Tohidi@pet.hw.ac.uk.

[†] Heriot-Watt University.

[‡] Ecole Nationale Supérieure des Mines de Paris.

10.1021/ie049843f CCC: $27.50
Published on Web 09/30/2004

Table 1. Measurement Principles of Direct Methods[11]

method	measuring principle
dew point mirror (chilled mirror)	temperature at which water or ice appears on a cooled surface
Karl Fischer titration	titration of absorbed water vapor with iodine
gravimetric hygrometer	increase in weight by absorption of water

solution theory of van der Waals and Platteeuw.[10] To check for the consistency of the new data, the experimental results are also compared with some correlations and models as well as other experimental data. The results are in good agreement demonstrating the reliability of techniques and model used for this work.

2. Review of the Experimental Set-Ups

Many techniques have been developed for the analysis of water content/water dew point in gases. This investigation of the principles of water content/water dew point measurement will cover a brief description of the commonly used methods. Some parts of the material in this report are based on those reported by van Rossum.[11]

The methods of gas water content/water dew point measurements can be divided into the following categories:

2.1. Direct Methods. Direct methods (absolute methods) utilize a direct relationship between the measured quantity and the water content/water dew point. In an ideal case no calibration is necessary. Therefore, these techniques also are called absolute techniques. Direct techniques consist of the following measurement techniques: (1) dew point mirror (chilled mirror), (2) Karl Fischer titration, and (3) gravimetric hygrometer. Measuring principles for the above techniques are given in Table 1.

Dew Point Mirror. The observation of dew point via a chilled surface, using either visual observation or instrumental detection of dew formation is a popular technique. For determination of the dew point with a dew point mirror, the gas is passed over a chilled metal mirror—a small high polished plate of gold, rhodium, platinum, or nickel in a pressure tight chamber. Historically, the cooling of the surface is accomplished with acetone and dry ice, liquid gases, mechanical refrigeration, and, more recently, by thermoelectric heat pumps. During cool down of the mirror, condensate forms on the mirror at dew point temperature. Condensate is detected by suitable means. The mirror temperature can be measured with a resistance thermometer directly attached to the back of the mirror. The mirror method is subject to contamination from heavy hydrocarbons and other components present in the gas. Depending on the kind of set-up, this method can measure dew point temperatures typically from 199.82 to 366.48 K with an accuracy better than 0.3 K. For estimating the water content, this method requires a psychometric chart giving the water content as a function of dew point.

Karl Fischer Titration. This method involves a chemical reaction between water and "*Karl Fischer Reagent*", which is typically a mixture of sulfur dioxide, iodine, pyridine, and methanol. For many years, this method was limited to laboratory use because of the equipment and chemicals required to carry out the determination. Recently, the newer Karl Fischer methods are faster and more convenient than the conventional methods for measuring water in hydrocarbons.

The Karl Fischer titration can be divided into two basic analytic groups with respect to dosing or production of iodine, respectively: (a) volumetric titration and (b) coulometric titration. During volumetric titration, the water-containing sample is solved in a suitable alcoholic solvent and is titrated with a Karl Fischer solution. Volumetric titration is applied for estimation of larger amounts of water typically in the range of 1 to 100 mg. Compared to that, coulometric Karl Fischer is a micromethod. Iodine is not dosed in the form of a solution but is directly used in an iodine containing solution via anodic oxidation. Due to its high analytic accuracy, it is suited for estimation of extremely low amounts of water (typically 10 μg to 50 mg). Therefore, for measuring water content of gases coulometric Karl Fischer titration is the preferred choice.

Gravimetric Hygrometer. Gravimetric hygrometer gives absolute water content, since the weight of water absorbed and the precise measurement of gas volume associated with the water determine the absolute water content of incoming gas. Gravimetric methods are of two types: *freezeout* and *adsorption*.

The freezeout technique can be used for gases containing light components (e.g. methane and ethane), because the condensation temperatures for these hydrocarbons are lower than that of water vapor. For the analysis of systems containing intermediate or heavy hydrocarbons (e.g. propane), the freezeout technique is very difficult because the intermediate or heavy hydrocarbons tend to condense along with water; as a consequence the separation of condensed phases is required before the amount of water can be determined. The small amounts of water and the loss that would occur on separation of the condensed hydrocarbons from the water rendered such a method of insufficient accuracy.

In the adsorption method, a test gas is pumped from a humidity generator through a drying train and a precision gas volume measuring system contained within a temperature-controlled bath. The precise measurements of the weight of water absorbed from the test gas and the associated volume of gas as measured at closely controlled temperature and pressure accurately defines the absolute water content of the test gas in units of weight per unit volume. This system has been chosen as the primary standard because the required measurements of weight, temperature, pressure, and volume can be made with extreme precision. The gravimetric hygrometer is a rather unwieldy instrument to use and in the low water content ranges may require up to 30 h per point. For this reason, the gravimetric hygrometer is not used for normal measurement purposes and would not be useful for industrial measurement or control.

2.2. Indirect Methods. With indirect methods, physical properties (e.g., conductivity, frequency etc., which are a function of water content) are measured from which dew point or water content can be calculated. Indirect methods, being relative methods, always require calibration. In other words, these methods can be useful if the relationship between water content (or water dew point) and the measured quantity can be determined empirically by comparison with a reference method. Such a reference method must be an absolute standard or a derivative of such a standard.

Table 2. Measurement Principles of Indirect Methods

method	measuring principle
spectroscopic	Water content is measured by detecting the energy absorption due to the presence of water vapor.
gas chromatography	Size of the peak is proportional to the amount of the analyzed sample.
electrolytic[a]	The current due to electrolysis of the absorbed water at known constant gas flow rate is directly proportional to water vapor concentration
capacitance[a]	Dielectric constant of aluminum oxide is a function of water vapor concentration
change in mass (quartz crystal)[a]	Hygroscopic coating adsorbs water; crystal resonant frequency is a function of mass and thus related to water vapor concentration
conductivity[a]	Salt/glycerol solution absorbs water vapor; conductivity is a function of water vapor concentration

[a] From ref 11.

Indirect methods can be divided into three subgroups: (1) spectroscopic: *(a) microwave, (b) infrared, and (c) laser;* (2) chromatographic: *(a) detection of water, (b) conversion to acetylene, and (c) conversion to hydrogen; and* (3) hygroscopic methods: *(a) electrolytic, (b) capacitance, (c) change in mass (quartz crystal), and (d) conductivity.* Measuring principles of the most popular indirect methods are given in Table 2.

Spectroscopic. Spectroscopic methods belong to optical instruments that measure the water content of gases by detecting the energy absorption to vaporized water. The basic unit consists of an energy source, a detector, an optical system for isolating specific wavelengths, and a measurement system for determining the attenuation of radiant energy caused by water vapor in the optical path.

These techniques for water content detection use normally radiations ranging from microwave (*MW*) frequencies through near-infrared (*NIR*). In general, the higher the frequency, the less the depth to which waves penetrates. Therefore, *MW* tends to be used more for bulk measurements, while *NIR* would be used for small samples. Because of the large differences in wavelengths, even though all the instruments are measuring the same parameter (water content), the mechanism of wave generation and detection differs. *MW* and *NIR* spectroscopic water content detectors cover a wide range of water content detectability, typically from 0.01% to over 99%. For many applications, the technologies overlap, and the choice of detector will depend on the size of the sample, process flow, degree of precision, and cost.

In contrast with the *MW* and *NIR* techniques, Tunable Diode Laser Absorption Spectroscopy (*TDLAS*) is an extremely sensitive technique used for measuring very low levels—as small as typically 100 parts per trillion (*ppt*). In a *TDLAS* water content analyzer, an infrared laser beam traverses the gas of interest, and changes in the intensity (due to water absorption) are measured. Path lengths are increased by a mirrored cell to bounce the laser light back and forth, thus improving the sensitivity. The gas of interest can be flowing through the chamber, giving real-time monitoring capability. In counterpart, these analyzers are expensive and require continual maintenance to care for the optical system. Absorption by gases can also cause severe interference to this method.

Chromatographic. *GC* is extensively used in various forms for water content determination. Methods vary in complexity from simple injection and separation by *GC* where the sensitivity is low to reaction with a reactant in *GC* where the water is converted into another compound, which exhibits a greater chromatographic response. The chromatographic technique allows analyzing water content on thermal conductivity detector (*TCD*), which is a quasi-universal detector. The most difficult part associated with this technique is the calibration of the detector response as a function of number of moles water in the sample.

The sample can be treated with calcium carbide to produce acetylene (acetylene can be detected on a high sensitivity detector i.e., a flame ionization detector (*FID*)) followed by determination of the gaseous product by *GC*. The determination of water using calcium carbide conversion is the subject of several studies,[12−19] and this technique has been proved to be accurate because the conversion of calcium carbide avoids absorption phenomena and allows a greater chromatographic response.

The reaction of water vapor with calcium carbide is as follows:

$$CaC_2 + 2H_2O \rightarrow Ca(OH)_2 + C_2H_2 \qquad (1)$$

However it is known that when calcium carbide is present in excess, a further slow reaction takes place between calcium carbide and calcium hydroxide yielding another molecule of acetylene as expressed by the following equation:

$$CaC_2 + Ca(OH)_2 \rightarrow 2CaO + C_2H_2 \qquad (2)$$

Nevertheless this method will not be accurate for the study of methanol containing samples as methanol reacts slowly with calcium carbide to form calcium methoxide and acetylene.

$$2CH_3OH + CaC_2 \rightarrow Ca(CH_3O)_2 + C_2H_2 \qquad (3)$$

An alternative to calcium carbide is to find another product, which suits the following conditions: Reactivity with water, complete decomposition of water in another compound, and no reactivity with C_1-C_4 hydrocarbons. Hydrides are compounds, which suit all conditions. Hydrides generate hydrogen according to the following reaction

$$MH_x + xH_2O \rightarrow M(OH)_x + xH_2 \qquad (4)$$

where M is a metal of valence x. The most suitable hydride to conduct some tests is lithium aluminum hydride,[20,21] because it can result in complete decomposition of water to hydrogen, as expressed by the following equation:

$$LiAlH_4 + 4H_2O \rightarrow Al(OH)_3 + LiOH + 4H_2 \qquad (5)$$

Hygroscopic Methods. The hygroscopic methods make use of sensors that respond to water vapor pressure in the gas phase. The surface properties of sensors are important. They will be sensitive to temperature variations, contaminants in the gas phase, coadsorption of other gaseous constituents, and past history of exposure.

Electrolytic. The electrolytic method is sometimes considered as being a direct method. This is only true if all of the water vapor flowing past the sensor is completely absorbed. For constant gas flow the amount of charge (current × time) is, by Faraday's law, a direct measure of water content. In practice, however, instruments based on this method require calibration because of the nonzero background current and because of the difficulty in ensuring that all of the water vapor is absorbed from the gas.

These sensors use a winding coated with a thin film of P_2O_5. As the desiccant absorbs incoming water vapor, an electrical potential is applied to the windings that electrolyzes the water to hydrogen and oxygen. The current consumed by the electrolysis determines the mass of water vapor entering the sensor. The flow rate and pressure of the incoming sample must be controlled precisely to maintain a standard sample mass flow rate into the sensor. Because the mechanism within the cell is complex, several additional phenomena may affect its operation.

Capacitance. The sensor is fabricated from a thin strip of pure aluminum. The aluminum strip is anodized in sulfuric acid, resulting in a layer of porous aluminum oxide on its surface. A layer of gold or noble metal is evaporated over the aluminum oxide. This sandwich of compounds is essentially a capacitor, with aluminum oxide layer as dielectric. Water vapor is rapidly transported through the noble metal layer and adsorbs onto the oxide as a function of partial pressure of water surrounding the sensor. The water molecules adsorbed on the oxide will cause a change in the dielectric constant of the sensor. A measure of the sensor impedance is a measure of the sample water partial pressure. Depending on the amount of water present in the stream, the impedance of the sensor can vary typically from 2 mega ohms to 50 kilo ohms. Thus the sensor produces a signal that is proportional to the amount of water content in the stream.

These sensors can detect water content levels typically from as low as 1 part per billion (*ppb*) to as high as approximately 200 000 parts per million (*ppm*). Slugs of liquid condensate, glycol, methanol, or water do not destroy it. It is designed for in-process mounting whenever possible, so as to eliminate the additional expense and complexity of sample conditioning.

The main limitation of the aluminum oxide sensor is its periodic calibrations against standards to determine if its response has changed due to contact with corrosive substances such as strong acids or bases.

Change in Mass (Quartz Crystal). This instrument compares the changes in frequency of a hydroscopically coated quartz oscillator. As the mass of the crystal changes due to adsorption of water vapor, its frequency changes correspondingly. The detector crystal is first exposed to the wet sample gas for a fixed period of time and then dried for a fixed period of time by a known dry reference gas. The difference in frequency between the wet and dry readings is proportional to the amount of water in the sample. The quartz crystal type water content analyzer can inherently respond very rapidly to small changes in water content.

The quartz crystal method is one of the best methods for clean and single component gases; however, it can suffer from coadsorption of other gas constituents by the hygroscopic coating and degradation of this coating.

This type of instrument is relatively expensive in commercial versions. In addition its flow sensitivity, susceptibility to damage by contact with water, and calibration dependence make it a difficult instrument to apply in general industrial applications.

Conductivity. The principle of measurement is based on the variation of the electrical conductivity of an unsaturated salt solution at varying gas water content. The saturation vapor pressure of an aqueous salt solution is lower than pure water. Therefore, the salt solution can absorb water from the surrounding medium until the vapor pressure of the salt solution and that of the measuring medium are in equilibrium. The absorption of water in the salt solution causes the electrical conductivity to decrease. The time required for equilibrium is a function of the size of the salt solution and the rate of mass transfer. At the same time, the temperature of the sensor influences the speed of response. To increase the speed of the sensor, one would have to construct very small sensors, so that the mass of the salt solution remains small. Because natural gases contain impurities, just a very small impurity would suffice (with very little measuring electrolyte) to destroy the sensor. The stability of the sensor would not be very large. Conversely, the use of a very large amount of electrolyte in the sensor would make the long-term stability very good, but the response speed would be relatively slow. A solution to these opposing demands has been found in the construction of sensors today.

A typical sensor consists of two high grade steel plates, which are electrically isolated from each other by a ceramic layer. Small holes are drilled in the layer package, whose inside walls are coated with a very thin film of a salt/glycerol electrolyte.

In this manner a more or less conductive connection between the two steel plates occurs. Several parallel wired single electrodes are created in this way. Because of the parallel wiring of the electrodes, the danger of becoming soiled is much smaller than with just one electrode, while the response speed is the same as for one tiny single electrode.

In normally polluted natural gas systems, the lifetime of the sensor is typically one year. The measuring accuracy after this time period is still sufficient, but the residue causes the sensors to be slower. For this reason, the sensors are replaced typically every three months. Afterward, the sensors can be cleaned and newly coated with electrolyte. The most severe problem in this method is that the salt solution can be washed off in the event of exposure to liquid water.

3. Literature Review of Water Content Data

Table 3 shows the majority of literature data from a study on the water content of the major constituents of natural gases. As can be seen, most of these data have been reported for the methane−water and carbon dioxide−water systems and at high temperature conditions (i.e., higher than 298 K in most cases). Only a few authors have studied systems at low temperature (in particular inside hydrate forming conditions), because of the very low water content and the difficulties associated with the analysis of water at such low concentrations.

4. Experimental Section

Based on the laboratory experience and on the existing laboratory equipment the *GC* method is selected in order to perform the analyses in this study.

Table 3. Literature Review of Water Content of Major Constituents of Natural Gases

component	reference	T_{min}/K	T_{max}/K	P_{min}/MPa	P_{max}/MPa
methane	Chapoy et al.[22]	283.08	318.12	0.992	35.090
	Dhima et al.[23]	298.15	298.15	≈2	≈35
	Althaus[24]	253.15	293.15	0.5	10
	Ugrozov[25]	310.95	377.55	2.53	70.93
	Yokoama et al.[26]	298.15	323.15	3	8
	Yarym-Agaev et al.[27]	298.15	338.15	2.5	12.5
	Gillespie and Wilson[28]	323.15	588.71	1.3786	16.8875
	Kosyakov et al.[29]	233.16	283.16	1.01	10.1
	Aoyagi et al.[30]	230.9	267.6	1.3786	10.34
	Kosyakov et al.[31]	233.15	273.15	1.013	10.13
	Aoyagi et al.[32]	240.0	270.0	3.4464	10.3393
	Sloan et al.[33]	249.98	280.017	6.8998	10.436
	Sharma[34]	NA[a]	NA[a]	NA[a]	NA[a]
	Rigby and Prausnitz[35]	298.15	373.15	2.35	9.35
	Lukacs and Robinson[36]	344.26	344.26	≈7.2	≈1.25
	Bukacek[1]	377.98	378.04	6.9411	68.7563
	Olds et al.[37]	310.93	510.93	2.672	68.856
ethane	Chapoy et al.[38]	278.08	303.11	0.323	4.63
	Althaus[24]	253.15	293.15	0.5	3
	Song and Kobayashi[39]	240.05	304.85	2.483	4.825
	Namiot[40]	344.25	377.55	2.53	70.93
	Song and Kobayashi[41]	240.05	304.85	2.483	4.825
	Sloan et al.[42]	259.1	270.5	3.45	3.45
	Bourrie and Sloan[43]	271.37	271.37	3.4464	3.4464
	Sparks and Sloan[44]	259.1	270.45	3.447	3.447
	Parrish et al.[45]	243.15	303.15	slightly above P^{sat}	slightly above P^{sat}
	Pollin et al.[46] (internal report)	NA[a]	NA[a]	NA[a]	NA[a]
	Coan and King[47]	298.15	373.15	2.2798	3.6376
	Anthony and McKetta[48]	310.93	410.87	2.5648	10.7956
	Anthony and McKetta[49]	310.87	377.71	3.4237	34.655
	Reamer et al.[50]	310.93	510.93	2.2112	68.2138
propane	Song and Kobayashi[39]	235.65	299.65	0.621	1.097
	Song and Kobayashi[41]	235.65	299.65	0.621	1.097
	Sloan et al.[42]	246.7	276.5	0.772	0.772
	Bourrie and Sloan[43]	264.15	264.15	3.4464	3.4464
	Sparks and Sloan[44]	246.66	276.43	0.772	0.772
	Parrish et al.[45]	243.15	303.15	slightly above P^{sat}	slightly above P^{sat}
	Pollin et al.[46] (internal report)	NA[a]	NA[a]	NA[a]	NA[a]
	Kahre[51] (internal report)	NA[a]	NA[a]	NA[a]	NA[a]
	Bukacek[1]	377.76	377.87	7.1755	67.38
	Kobayashi and Katz[52]	278.872	422.04	0.5666	19.32
	Kobayashi[53]	NA[a]	NA[a]	NA[a]	NA[a]
	Poettmann and Dean[54]	288.71	359.26	NA[a]	NA[a]
	Chaddock[55]	299.82	369.65	1.1373	17.2321
	Perry[56]	310.93	310.93	1.351	1.351
	Hachmuth[57]	310.93	310.93	1.351	1.351
	McKetta and co-workers[58, 59]	NA[a]	NA[a]	NA[a]	NA[a]
butane	Parrish et al.[45]	243.15	303.15	slightly above P^{sat}	slightly above P^{sat}
	Anthony and McKetta[48]	344.26	344.26	0.856	0.8685
	Wehe and McKetta[60]	310.87	410.93	0.3591	3.389
	Reamer et al.[61]	310.93	510.93	0.1379	68.929
	Brooks et al.[62]	310.93	377.59	7.27	69.3766
	Black et al.[63]	278.15	294.15	0.27	0.65
	McKetta and Katz[64]	NA[a]	NA[a]	NA[a]	NA[a]
	Reamer et al.[65]	310.93	425.15	0.3615	4.394
	McKetta and co-workers[58, 59]	NA[a]	NA[a]	NA[a]	NA[a]
carbon dioxide	Dohrn et al.[66]	323.15	323.15	10.1	30.1
	King et al.[67]	288.15	313.15	5.17	20.27
	D'Souza et al.[68]	323.15	348.15	10.133	15.200
	Müller et al.[69]	373.15	473.15	0.325	8.11
	Briones et al.[70]	323.15	323.15	6.82	17.68
	Nakayama et al.[71]	298.2	298.2	3.63	10.99
	Song and Kobayashi[72]	245.15	304.21	0.69	13.79
	Song and Kobayashi[73]	255.35	298.15	3.45	13.79
	Song et al.[74]	255.35	298.15	3.45	13.79
	Gillespie et al.[75]	289.15	533.15	0.7	13.8
	Gillespie and Wilson[28]	288.71	533.15	0.6893	20.265
	Chrastil[76]	323.15	353.15	10.1325	25.33125
	Zawisza and Malesinska[77]	373.15	473.15	0.466	6.692
	Kobayashi et al.[78] (internal report)	NA[a]	NA[a]	NA[a]	NA[a]
	Coan and King[47]	298.15	373.15	1.7327	5.1473
	Takenouchi and Kennedy[79]	383.15	623.15	10	300
	Tödheide and Franck[80]	323.15	623.15	20.0	350.0
	Malinin[81]	473.15	603.15	20.265	60.795
	Sidorov et al.[82]	273.15	348.15	2.53312	30.3975
	Stone[83]	244.15	295.75	1.5199	6.0795
	Wiebe and Gaddy[84]	298.15	348.15	0.101325	70.9275
	Pollitzer and Strebel[85]	323	343.2	3.0904	8.8153

Table 3. (Continued)

component	reference	T_{min}/K	T_{max}/K	P_{min}/MPa	P_{max}/MPa
nitrogen	Althaus[24]	248.15	293.15	0.5	10
	Kosyakov et al.[29]	233.16	293.16	1.01	12.12
	Gillespie and Wilson[86]	310.93	588.71	0.345	13.786
	Kosyakov et al.[87]	233.15	273.15	1.013	10.13
	Maslennikova et al.[88]	298.15	623.15	5.06625	50.6625
	Rigby and Prausnitz[35]	298.15	373.15	2.1086	10.1518
	Namiot and Bondareva[89]	310.95	366.45	0.34	13.79
	Bukacek[1]	377.65	378.09	6.9825	68.2738
	Sidorov et al.[82]	373.15	373.15	5.06625	40.530
	Saddington and Krase[90]	323.15	503.15	10.1325	30.3975
	Bartlett[91]	323.15	323.15	10.1325	101.325
hydrogen sulfide	Gillespie and Wilson[92]	310.93	588.71	4.1357	20.6786
	Gillespie et al.[75]	310.15	588.15	NA[a]	10
	Gillespie and Wilson[86]	310.93	588.71	0.3446	13.7857
	Lee and Mather[93]	363.15	423.15	1.5	3.5
	Selleck et al.[94]	302.65	444.26	0.6893	34.4643
	Wright and Maass[95]	278.15	333.15	0.03660	0.4942

[a] N.A.: Not available.

4.1. Materials. Methane and ethane were purchased by *Messer Griesheim* with a certified purity greater than 99.995 volume percent for both gases. Helium from *Air Liquide* is pure grade with traces of water (3 *ppm*) and of hydrocarbons (0.5 *ppm*). Furthermore, helium was dried by means of molecular sieves placed at the outlet of the cylinder.

4.2. Apparatus. The apparatus used in this work (Figure 1) is based on a static-analytic method with vapor phase sampling. This apparatus is similar to that described by Chapoy et al.[22,38]

The phase equilibrium is achieved in a cylindrical cell made of *Hastelloy HC276*, the cell volume is about 34 cm^3 (internal diameter = 25 mm and high = 69.76 mm),

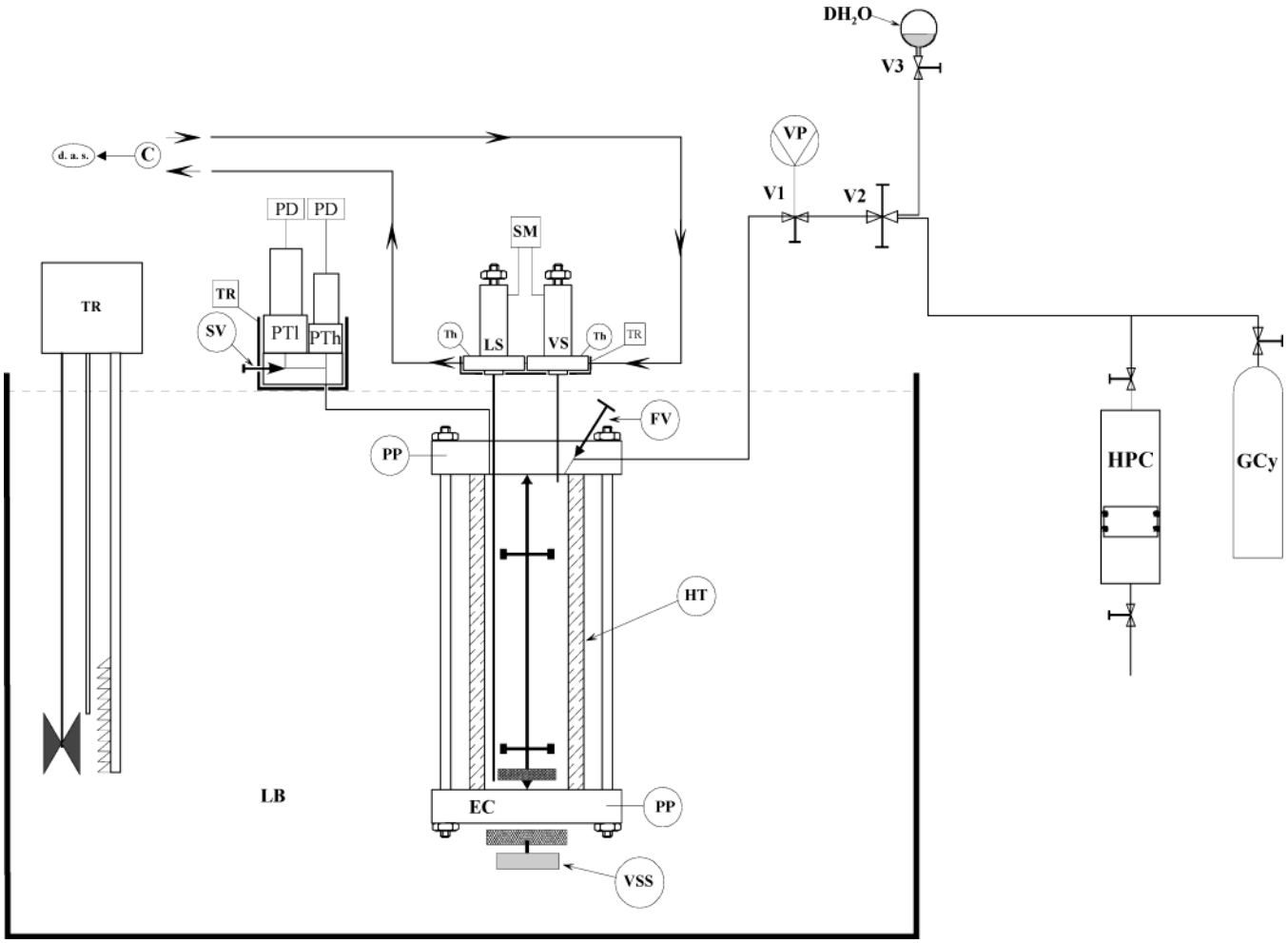

Figure 1. Flow diagram of the equipment.[22,38] C: carrier gas; d.a.s: data acquisition system; DH_2O: degassed water; EC: equilibrium cell; FV: feeding valve; GCy: gas cylinder; HPC: high-pressure compressor; HT: Hastelloy tube; LB: liquid bath; LS: liquid sampler; PD: pressure display; PP: platinum resistance thermometer probe; PTh and PTl: high- and low-pressure transducers; SM: sampler monitoring; SV: special valve; Th: thermocouple; TR: temperature regulator; Vi: valve i; VS: vapor sampler; VSS: variable speed stirrer; VP: vacuum pump.

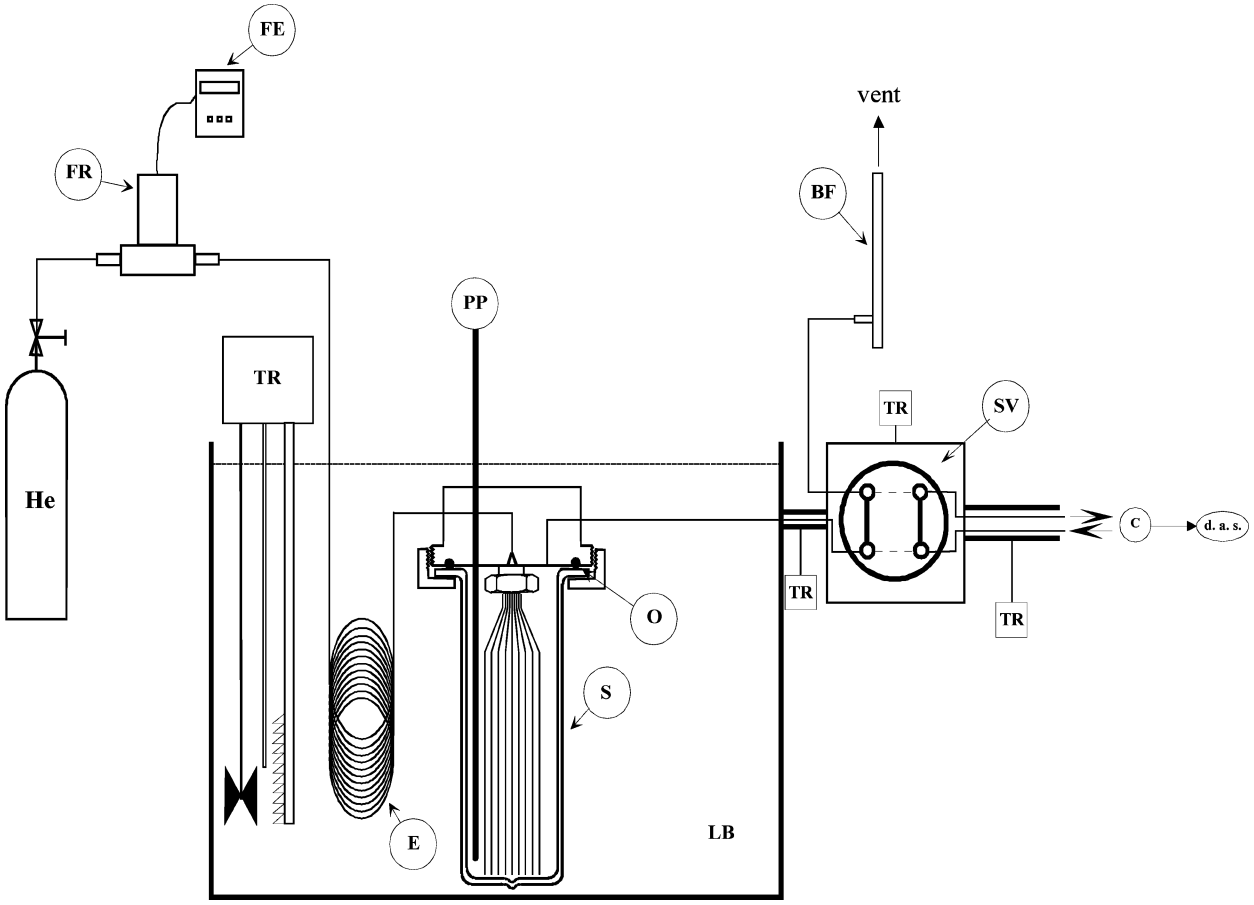

Figure 2. Flow diagram of the calibration circuit.[22,38] BF: bubble flowmeter; C: carrier gas; d.a.s: data acquisition system; E: thermal exchanger; FE: flow rate electronic; FR: flow rate regulator; LB: liquid bath; O: o'ring; pp: platinum resistance thermometer probe; S: saturator; SV: internal loop sampling valve; TR: temperature regulator.

and it can be operated under a pressure of up to 40 MPa and from 223.15 to 473.15 K. The cell is immersed into an *ULTRA-KRYOMAT LAUDA* constant-temperature liquid bath that controls and maintains the desired temperature within ± 0.01 K. To perform accurate temperature measurements in the equilibrium cell and to check for thermal gradients, two *Pt100* Platinum Resistance Thermometer Devices measure temperature in two locations corresponding to the vapor and liquid phases connected to an *HP* data acquisition unit (*HP34970A*). These two *Pt100* connected to an *HP* data acquisition unit (*HP34970A*) are carefully and periodically calibrated against a 25 ohms reference platinum resistance thermometer (*TINSLEY* Precision Instruments). The resulting uncertainty is not higher than ± 0.02 K. The 25 ohms reference platinum resistance thermometer was calibrated by the *Laboratoire National d'Essais* (Paris) based on the 1990 International Temperature Scale (*ITS 90*). Pressures are measured by means of two *Druck* pressure transducers (type *PTX 610* range 0−30 MPa and type *PTX611*, range: 0−1.5 MPa) connected to the same *HP* data acquisition unit (*HP34970A*) as the two *Pt100*; the pressure transducers are maintained at constant temperature (temperature higher than the highest temperature of the study) by means of a homemade air-thermostat, which is controlled by a *PID* regulator (*WEST* instrument, model 6100).

Both pressure transducers are calibrated against a dead weight balance (*Desgranges & Huot 5202S, CP* 0.3 to 40 MPa, *Aubervilliers,* France). The uncertainty in the pressure measurements is estimated to be within ± 0.5 kPa for the 0−1.6 MPa pressure transducer in a range up to 2.5 MPa and ± 5 kPa for the 0−30 MPa pressure transducer from 2.5 to 38 MPa. The *HP* online data acquisition system is connected to a personal computer through a *RS-232* interface. This complete system allows real time readings and records of temperatures and pressures all along the different isothermal runs.

The analytical work was carried out using a *GC* (*VARIAN model CP-3800*) equipped with two detectors connected in series, a *TCD* and a *FID*, connected to a data acquisition system (*BORWIN* ver. 1.5, from *JMBS, Le Fontanil*, France). The analytical column is *HayeSep C 80/100 Mesh* (*SilcoSteel* tube, length: 2 m, diameter: 1/8”). The *FID* was utilized to detect the hydrocarbons. It was repeatedly calibrated by introducing known amounts of methane and ethane through a gas syringe in the injector of the *GC*. The methane and ethane calibration uncertainty are estimated to be within ± 1%. For *TCD* calibration purposes, a dilutor/saturator apparatus is used with a specific calibration circuit (Figure 2). The cell of the dilutor is immersed in a liquid thermoregulated bath. Helium is bubbled through the dilutor cell filled with water to be saturated, before entering the *GC* through a 5 μL internal loop injection valve. In using the dilutor and a loop injection valve, a well-defined amount of water can be injected into the *GC*.

The calculation of the amount of water is carried out using equilibrium and mass balance relations. At thermodynamic equilibrium, the fugacity of water is the same in both vapor and liquid phases, and the water

mol fraction remains constant when the saturated gas is heated in the internal valve; an exact relationship can be obtained

$$f_w^L = f_w^V \tag{6}$$

with

$$f_w^L = f_w^{Lref} \times \gamma_w^L \times x_w \tag{7}$$

for a pressurized liquid

$$f_w^{L_{\text{ref}}} = f_w^{sat} \exp\left(\int_{P^{sat}}^{P} \left(\frac{v^L}{RT}\right) dP\right) \tag{8}$$

assuming the Poynting correction:

$$f_w^{L_{\text{ref}}} = f_w^{sat} \exp\left(\left(\frac{v^L}{RT}\right)(P - P^{sat})\right) \tag{9}$$

Equation 6 becomes

$$f_w^V = \gamma_w^L x_w f_w^{sat} \exp\left(\left(\frac{v^L}{RT}\right)(P - P^{sat})\right) \tag{10}$$

$$f_w^V = \gamma_w^L x_w P_w^{sat} \phi_w^{sat} \exp\left(\left(\frac{v^L}{RT}\right)(P - P^{sat})\right) \tag{11}$$

because

$$P_w^{sat} \phi_w^{sat} = f_w^{sat} \tag{12}$$

on the other hand

$$f_w^V = \phi_w^V P_{dilutor} y_w \tag{13}$$

thus

$$y_w = \gamma_w^L x_w \frac{P_w^{sat} \phi_w^{sat}}{P_{dilutor} \phi_w^V} \exp\left(\left(\frac{v^L}{RT}\right)(P - P^{sat})\right) \tag{14}$$

with

$$y_w = \frac{n_w}{n_T} \tag{15}$$

An exact relationship is obtained

$$n_w = \gamma_w^L x_w \frac{P_w^{sat} \phi_w^{sat}}{P_{dilutor} \phi_w^V} \left(\frac{P.Vol}{ZRT}\right)^{loop} \exp\left(\left(\frac{v^L}{RT}\right)(P - P^{sat})\right) \tag{16}$$

In the above relations, f, γ, x, v, R, T, P, ϕ, y, n, Z, and Vol are fugacity, activity coefficient, mol fraction in the liquid phase, molar volume, universal gas constant, temperature, pressure, fugacity coefficient, mol fraction in the vapor phase, number of moles, compressibility factor, and volume of the loop, respectively. The superscripts and subscripts L, V, *ref*, *sat*, *loop*, w, T, and *dilutor* correspond to the liquid phase, vapor phase, reference state, saturation state, loop, water, total, and dilutor, respectively.

To minimize the adsorption phenomenon, the internal injection valve was maintained at high temperature, i.e., 523.15 K. The experimental accuracy of the *TCD* water calibration (from 9×10^{-10} mol to 1.2×10^{-8}) is estimated in the worst case at ± 5%. An example of a typical water calibration curve as well as experimental uncertainties of the *TCD* water calibration are available in ref 38.

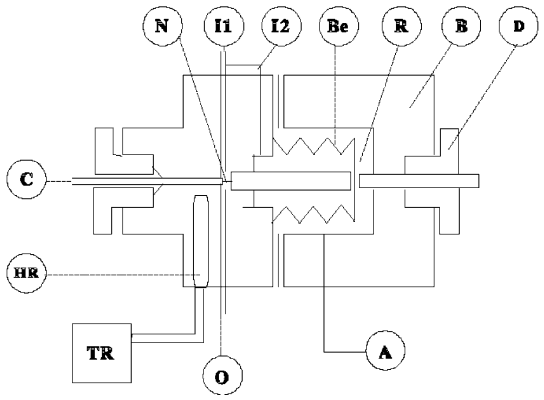

Figure 3. Flow diagram of the sampler-injector. A: air inlet; B: body; Be: bellow; C: capillary tube; D: differential screw; N: micro needle; HR: heating resistance; R: expansion room; TR: thermal regulator; I1, I2: carrier gas inlet; O: carrier gas outlet.

Table 4. Critical Properties and Acentric Factors[97]

compound	P_c/MPa	T_c/K	v_c/m^3.kg mol^{-1}	ω
water	22.048	647.30	0.0560	0.3442
methane	4.604	190.58	0.0992	0.0108
ethane	4.880	305.42	0.1479	0.09896

4.3. Experimental Procedure. The equilibrium cell and its loading lines are evacuated down to 0.1 Pa, and the necessary quantity of the preliminary degassed water (approximately 10 cm^3) is introduced using an auxiliary cell. Afterward, the desired amount of methane is introduced into the cell directly from the cylinder or via a gas compressor. The sampling is carried out using a capillary sampler injector[96] (Figure 3). Two capillary sampler-injectors, for each phase, are connected to the cell by two 0.1 mm internal diameter capillary tube. The withdrawn samples are swept to a *Varian 3800 GC* for analysis. For each equilibrium condition, at least 10 points are withdrawn using the pneumatic samplers *ROLSI* and analyzed in order to check for measurement repeatability. As the volume of the withdrawn samples is very small compared to the volume of the vapor phase present in the equilibrium cell, it is possible to withdraw many samples without disturbing the phase equilibrium.

5. Thermodynamic Model

5.1. Pure Compound Properties. The critical temperature (T_C), critical pressure (P_C), critical volume (v_C), and acentric factor (ω), for each of the pure compounds are provided in Table 4.

5.2. Description of the Model. A detailed description of the model is given in the Appendix. Briefly, a thermodynamic model based on uniformity of fugacity of each component throughout all the phases[98,99] is extended to model the equilibrium conditions. The *VPT*−*EoS*[8] with *NDD* mixing rules[9] is used to determine component fugacities in fluid phases. This combination has proved to be a strong tool in modeling systems with polar as well as nonpolar compounds.[9] The fugacity of ice is rigorously calculated by correcting the saturation fugacity of water at the same temperature by using the Poynting correction. The hydrate phase is modeled using the solid solution theory of van der Waals

Table 5. Kihara Potential Parameters for Methane[a]

compound	α/Å	σ^{*b}/Å	(ϵ/k')/K
methane	0.2950	3.2512	153.69

[a] From ref 100. [b] $\sigma^* = \sigma - 2\alpha$.

Table 6. Thermodynamic Reference Properties for Structure-I (*sI*) Hydrates

structure	I
$\Delta\mu_w^0$/(J mol^{-1})	1297[d]
Δh_w^0/(J mol^{-1})[a]	1389[d]
Δv_w/(cm^3 mol^{-1})[b]	3.0[e]
ΔC_{pw}^0/(J mol^{-1} K^{-1})[c]	−37.32 [f]

[a] In the liquid water region subtract 6009.5 J/mol from Δh_w^0. [b] In the liquid water region add 1.601 cm^3/mol to Δv_w. [c] Values to be used in $\Delta C_{pw} = \Delta C_{pw}^\circ + 0.179(T-T_0)$. [d] Reference 105. [e] Reference 102. [f] Reference 104.

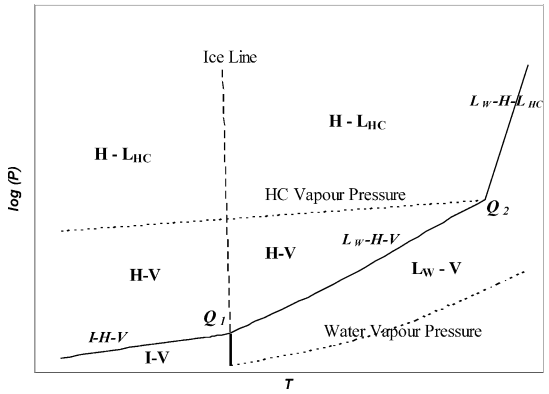

Figure 4. Typical pressure−temperature diagram for a water (limiting reactant) − single (pure) hydrocarbon system.[24]

and Platteeuw.[10] The Kihara model for spherical molecules is applied to calculate the potential function for compounds forming hydrate phases. These parameters are taken from ref 100 (Table 5). Table 6 shows thermodynamic reference properties for hydrates used in modeling.

Figure 4 shows a typical pressure-temperature diagram for the water−hydrocarbon system (pure gas and water as limiting component). As can be seen, for *H*−*V* equilibria, the temperature must be below the three-phase liquid water−hydrate−vapor (*L*$_w$−*H*−*V*) or ice−hydrate−vapor (*I*−*H*−*V*) temperature at a given pressure. Alternatively the pressure must be above the three-phase *L*$_w$−*H*−*V* or *I*−*H*−*V* pressure at a given temperature.[106] Consequently, for ice−vapor (*I*−*V*) equilibrium the temperature must be above the *I*−*V*−*H* temperature at a given pressure or the pressure must be below the *I*−*H*−*V* pressure at a given temperature. Also, for liquid water−vapor (*L*$_w$−*V*) equilibrium the temperature must be above the *L*$_w$−*V*−*H* temperature at a given pressure or the pressure must be below the *L*$_w$−*H*−*V* pressure at a given temperature.

6. Results and Discussion

A preliminary study shows that most of the existing *EoSs* were developed at relatively high-temperature conditions. Therefore, the *EoS* may not cover low-temperature conditions.[24] Different attempts have been made to solve this problem. Some investigators developed new alpha functions for appropriate *EoS*, particularly Peng−Robinson *(PR) EoS* and some of them relaxed the alpha function for water, to improve the predicted water fugacity. Exact prediction of the water vapor pressure has an important effect on the phase behavior of wet gases.[24] The calculated results significantly depend on the temperature dependency of the alpha function. This function is generally developed as a function of reduced temperature and acentric factor. Anderko[107] mentioned that the acentric factor is not a characteristic parameter for polar substances. This fact may lead to undesired results, when using the acentric factor in the alpha function for the polar substances. To improve the predicted water fugacity in this study, the alpha function for water in the *VPT*−*EoS*,[8] $\alpha_w(T_r)$, is relaxed, using experimental water vapor pressure data in the range of 258.15 to 374.15 K, as implemented by Tohidi-Kalorazi[100] (eq A.11).

Table 7. BIPs for the *VPT*−*EoS*[8] and *NDD* Mixing Rules[9] [a]

system	k_{w-g}	$l_{w-g}{}^1$	$l_{w-g}{}^2 \times 10^4$
methane−water[b]	0.5044	1.8302	51.72
ethane−water[c]	0.4974	1.4870	45.40

[a] w: water, g: gas. [b] From ref 108. [c] From ref 100.

To further develop the thermodynamic model, the binary interaction parameters (*BIP*s) between methane and water and also ethane and water are set directly to those reported by Chapoy et al.[108] and Tohidi-Kalorazi.[100] Table 7 shows the *BIP*s used in this work.

The water content experimental and predicted data are reported in Tables 8 and 9 and plotted in Figure 5. The corresponding values of the absolute deviation (*AD*) are given in the tables. The *AD*s are defined by eq 17

$$AD = \left|\frac{y_{i,exp} - y_{i,prd}}{y_{i,exp}}\right| \qquad (17)$$

where $y_{i,exp}$ is the measured water content and $y_{i,prd}$ is the predicted water content.

In Tables 8 and 9, the water content measurements of the methane and ethane systems have been compared with other predictive methods. As can be seen, the new experimental data are in good agreement with predictions of this model and *Bukacek* correlation[1] as well as the *AQUAlibrium* model.[109] It should be noted that the water vapor pressure for Ideal model, Ideal model + Poynting correction, and Bukacek correlation[1] has been calculated using the correlation given by Daubert and Danner.[110] For further investigation, the data are compared with the available data in the literature. As illustrated in Figure 5, the results are consistent with those of all the authors.

7. Conclusions

Accurate water content data especially at low-temperature conditions are necessary for industrial applications involving water−hydrocarbon systems. For this purpose, a review was conducted on the commonly used experimental methods for measuring water content/water dew point of gases as well as the experimental data in the literature.

The investigation showed that most of the existing data have been reported at high-temperature conditions, and the data reported at low-temperature conditions are scattered and dispersed.

Table 8. Experimental and Predicted Water Contents (Mol Fraction × 1000) in Water + Methane System

P/MPa	*T*/K	exptl	this model	Ideal model	Ideal model + Poynting correction	Bukacek correlation[1]	AQUA-librium model [109]	*AD%*, this model	*AD%*, Ideal model	*AD%*, Poynting correction	*AD%*, Bukacek correlation[1]	*AD%*, AQUA-librium model [109]
1.147	282.98	1.143	1.114	1.058	1.067	1.15	1.112	2.54	7.44	6.65	0.61	2.71
1.005	283.08	1.240	1.272	1.216	1.225	1.308	1.277	2.58	1.94	1.21	5.48	2.98
1.003	283.15	1.260	1.280	1.224	1.233	1.316	1.286	1.59	2.86	2.14	4.44	2.06
1.000	288.11	1.780	1.775	1.701	1.714	1.819	1.783	0.28	4.44	3.71	2.19	0.17
1.005	288.15	1.770	1.771	1.697	1.710	1.815	1.779	0.06	4.12	3.39	2.54	0.51
2.051	293.01	1.170	1.230	1.131	1.148	1.279	1.241	5.13	3.33	1.88	9.32	6.07
0.992	293.01	2.410	2.434	2.338	2.355	2.486	2.445	1.00	2.99	2.28	3.15	1.45
0.510	293.01	4.640	4.642	4.547	4.564	4.695	4.654	0.04	2.00	1.64	1.19	0.30
0.990	293.11	2.400	2.454	2.357	2.374	2.506	2.465	2.25	1.79	1.08	4.42	2.71
0.563	297.97	5.690	5.694	5.571	5.594	5.756	5.71	0.07	2.09	1.69	1.16	0.35
1.697	298.00	1.959	1.979	1.852	1.875	2.037	1.993	1.02	5.46	4.29	3.98	1.74
0.608	298.01	5.193	5.295	5.171	5.194	5.357	5.31	1.96	0.42	0.02	3.16	2.25
2.846	298.01	1.218	1.236	1.105	1.128	1.290	1.25	1.48	9.28	7.39	5.91	2.63
1.010	298.11	3.270	3.258	3.132	3.155	3.318	3.272	0.37	4.22	3.52	1.47	0.06
1.030	303.11	4.400	4.278	4.115	4.145	4.346	4.296	2.77	6.48	5.80	1.23	2.36
0.990	308.11	5.820	5.883	5.675	5.714	5.961	5.907	1.08	2.49	1.82	2.42	1.49
1.090	313.12	7.340	7.032	6.766	6.817	7.117	7.061	4.20	7.82	7.13	3.04	3.80

Table 9. Experimental and Predicted Water Content (Mol Fraction × 1000) in Water + Ethane System

P/MPa	T/K	exptl	this model	Ideal model	Ideal model + Poynting correction	Bukacek correlation [1]	AQUA-librium model [109]	AD% this model	AD% Ideal model	AD% Poynting correction	AD% Bukacek correlation[1]	AD% AQUA-librium model [109]
0.506	282.93	2.442	2.412	2.390	2.399	2.482	2.417	1.23	2.13	1.76	1.64	1.02
1.859	288.11	1.031	0.933	0.915	0.9279	1.033	0.942	9.51	11.25	10.00	0.19	8.63
1.049	292.95	2.204	2.236	2.203	2.220	2.350	2.245	1.45	0.05	0.73	6.62	1.86
2.990	293.10	0.832	0.7839	0.7799	0.7974	0.9285	0.798	5.78	6.26	4.16	11.60	4.09
1.926	293.10	1.305	1.2352	1.211	1.228	1.359	1.246	5.35	7.20	5.90	4.14	4.52

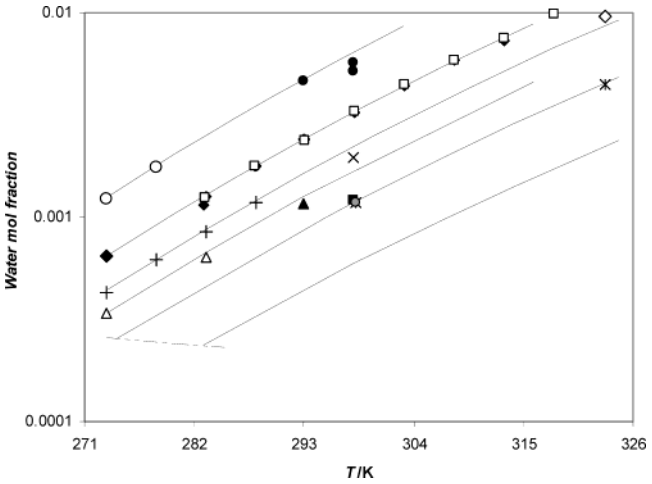

Figure 5. Water content of methane as a function of temperature at different pressures. (○) data at 0.500 MPa;[24] (●) data at 0.510, 0.563, and 0.608 MPa (this work); (◆) data from 0.990 up to 1.147 MPa (this work), (□) data from 0.992 up to 1.100 MPa;[22] (+) data at 1.500 MPa;[24] (×) data at 1.697 MPa (this work); (◇) data at 1.379 MPa;[28] (△) data at 2.030 MPa;[29] (▲) data at 2.051 (this work); (■) data at 2.846 MPa (this work); (*) data at 3.000 MPa;[26] (●) data at 3.051 MPa;[35] solid lines, predicted with the *VPT−EoS*[8] and *NDD* mixing rules [9] at 0.5, 1, 1.5, 2, 3, and 7 MPa, respectively; dashed line, hydrate formation conditions predicted by using the solid solution theory of van der Waals and Platteeuw.[10]

New experimental data on the water contents of methane and ethane were generated at different temperature and pressure conditions using a static-analytic apparatus, taking advantage of a high-pressure capillary sampler. The new experimental data were compared with predictions of an in-house thermodynamic model as well as other predictive methods. The predictions were in good agreement with the experimental data, demonstrating the reliability of the techniques and model used in this work.

Acknowledgment

The financial support by the European Infrastructure for Energy Reserve Optimization (*EIERO*), the Gas Processor Association (*GPA*), and a joint industrial project supported by *Shell*, *TOTAL*, *Statoil*, and *Petrobras* provided the opportunity for this joint work, which is gratefully acknowledged.

Appendix

Description of the Model. A general phase equilibrium model based on equality of fugacity of each component throughout all the phases[98,99] is extended to model the equilibrium conditions. The *VPT−EoS* [8] with *NDD* mixing rules[9] is used to determine component fugacities in fluid phases. This *EoS*[8] is given by

$$P = \frac{RT}{v-b} - \frac{a}{v(v+b)+c(v-b)} \tag{A.1}$$

with

$$a = \bar{a}\alpha(T_r) \tag{A.2}$$

$$\bar{a} = \frac{\Omega_a R^2 T_c^{\,2}}{P_c} \tag{A.3}$$

$$b = \frac{\Omega_b R T_c}{P_c} \tag{A.4}$$

$$c = \frac{\Omega_{c^*} R T_c}{P_c} \tag{A.5}$$

$$\alpha(T_r) = [1 + F(1 - T_r^{\,\Psi})]^2 \tag{A.6}$$

where $\psi = 0.5$. The subscripts *c* and *r* denote critical and reduced properties, respectively.

The coefficients Ω_a, Ω_b, Ω_{c*}, and F are given by

$$\Omega_a = 0.66121 - 0.76105Z_c \quad (A.7)$$

$$\Omega_b = 0.02207 + 0.20868Z_c \quad (A.8)$$

$$\Omega_{c*} = 0.57765 - 1.87080Z_c \quad (A.9)$$

$$F = 0.46283 + 3.58230(\omega Z_c) + 8.19417(\omega Z_c)^2 \quad (A.10)$$

where Z_c is the critical compressibility factor, and ω is the acentric factor. Tohidi-Kalorazi[100] relaxed the alpha function for water, $\alpha_w(T_r)$, using experimental water vapor pressure data in the range of 258.15 to 374.15 K, to improve the predicted water fugacity:

$$\alpha_w(T_r) = 2.4968 - 3.0661T_r + 2.7048{T_r}^2 - 1.2219{T_r}^3 \quad (A.11)$$

The above relation is used in the present work.

In this work the *NDD* mixing rules developed by Avlonitis et al.[9] are applied to describe mixing in the *a*-parameter

$$a = a^C + a^A \quad (A.12)$$

where a^C is given by the classical quadratic mixing rules as follows

$$a^C = \sum_i \sum_j x_i x_j a_{ij} \quad (A.13)$$

and b, c, and a_{ij} parameters are expressed by

$$b = \sum_i x_i b_i \quad (A.14)$$

$$c = \sum_i x_i c_i \quad (A.15)$$

$$a_{ij} = (1 - k_{ij})\sqrt{a_i a_j} \quad (A.16)$$

where k_{ij} is the *BIP*.

The term a^A corrects for asymmetric interaction, which cannot be efficiently accounted for by classical mixing rules

$$a^A = \sum_p {x_p}^2 \sum_i x_i a_{pi} l_{pi} \quad (A.17)$$

$$a_{pi} = \sqrt{a_p a_i} \quad (A.18)$$

$$l_{pi} = {l_{pi}}^1 - {l_{pi}}^2(T - T_0) \quad (A.19)$$

where p is the index of polar components and l represents the binary interaction parameter for the asymmetric term.

Using the *VPT*−*EoS*[8] and the *NDD* mixing rules,[9] the fugacity of each component in all fluid phases is calculated from

$$ln\phi_i = \frac{1}{RT}\int_{\bar{V}}^{\infty}\left[\left(\frac{\partial P}{\partial n_i}\right)_{T,\bar{V},n_{j\neq i}} - RT/\bar{V}\right]d\bar{V} - ln\ Z \text{ for } i = 1, 2, ..., nc \quad (A.20)$$

$$f_i = x_i \phi_i P \quad (A.21)$$

where $\bar{V}$ and nc are the volume and number of components, respectively.

The fugacity of ice is rigorously calculated by correcting the saturation fugacity of water at the same temperature by using the Poynting correction

$$f^I_w = \phi^{sat}_w P^{sat}_I \exp\left(\frac{v_I(P - P^{sat}_I)}{RT}\right) \quad (A.22)$$

where f^I_w is the fugacity of water in the ice phase, ϕ^{sat}_w is the water fugacity coefficient in the vapor phase at pressure equal to the ice vapor pressure, P^{sat}_I is the ice vapor pressure, and v_I is the ice molar volume, respectively.

The ice molar volume, v_I, is calculated using the following expression[100]

$$v_I = 19.655 + 0.0022364 \times (\text{T-273.15}) \quad (A.23)$$

where v_I and T are in $cm^3/gmol$ and *Kelvin*, respectively. The ice vapor pressure, P^{sat}_I, is calculated using[100]

$$log(P^{sat}_I) = -1033/T + 51.06 \times \log(\text{T}) - 0.09771 \times \text{T} + 7.036 \times 10^{-5} \times T^2 - 98.51 \quad (A.24)$$

where T and P^{sat}_I are in *Kelvin* and *mmHG*, respectively.

The fugacity of water in the hydrate phase, f^H_w, is given by[101]

$$f^H_w = f^\beta_w \exp\left(-\frac{\Delta\mu^{\beta-H}_w}{RT}\right) \quad (A.25)$$

where f^β_w is the fugacity of water in the empty hydrate lattice. $\Delta\mu^{\beta-H}_w$ is the chemical potential difference of water between the empty hydrate lattice, μ^β_w, and the hydrate phase, μ^H_w, which is given by the following equation[10,101,102]

$$\Delta\mu^{\beta-H}_w = \mu^\beta_w - \mu^H_w = RT\sum_m \bar{\nu}_m \ln(1 + \sum_j C_{mj} f_j) \quad (A.26)$$

where $\bar{\nu}_m$ is the number of cavities of type m per water molecule in the unit cell, f_j is the fugacity of the gas component j, and C_{mj} is the Langmuir constant, which is a function of temperature according to the relation[10,101,102]

$$C_{mj}(T) = \frac{4\pi}{k'T}\int_0^\infty \exp\left(-\frac{w(r)}{k'T}\right) r^2 dr \quad (A.27)$$

where k' is Boltzmann's constant and $w(r)$ is the spherically symmetric cell potential in the cavity, with r measured from the center depending on the intermolecular potential function chosen for describing the encaged guest−water interaction. In the present work, the Kihara potential function with a spherical core is used[102]

$$\Gamma(r) = \infty \qquad r \leq 2\alpha \quad (A.28)$$

$$\Gamma(r) = 4\epsilon\left[\left(\frac{\sigma^*}{r - 2\alpha}\right)^{12} - \left(\frac{\sigma^*}{r - 2\alpha}\right)^6\right] r > 2\alpha$$

where $\Gamma(r)$ is the potential energy of interaction between two molecules when the distance between their centers is equal to r. ϵ is the characteristic energy, α is the

radius of the spherical molecular core, and $\sigma^* = \sigma - 2\alpha$ where σ is the collision diameter, i.e., the distance where $\Gamma = 0$. The Kihara potential parameters, α, σ, and ϵ, are taken from ref 100 (Table 5). Based on the chosen potential energy function the spherically symmetric cell potential in the cavities (eq A.27) needs to be derived. McKoy and Sinanoglu[103] summed up all these guest−water binary interactions inside the cell to yield an overall cell potential[102,103]

$$w(r) = 2z\epsilon\left[\frac{(\sigma^*)^{12}}{\bar{R}^{11}r}\left(\delta^{10} + \frac{\alpha}{\bar{R}}\delta^{11}\right) - \frac{(\sigma^*)^6}{\bar{R}^5 r}\left(\delta^4 + \frac{\alpha}{\bar{R}}\delta^5\right)\right] \tag{A.29}$$

$$\delta^{\bar{N}} = \frac{1}{\bar{N}}\left[\left(1 - \frac{r}{\bar{R}} - \frac{\alpha}{\bar{R}}\right)^{-\bar{N}} - \left(1 + \frac{r}{\bar{R}} - \frac{\alpha}{\bar{R}}\right)^{-\bar{N}}\right] \tag{A.30}$$

where z is the coordination number of the cavity, that is the number of oxygen molecules at the periphery of each cavity, $\bar{R}$ is the cavity radius, r is the distance of the guest molecule from the cavity center, and $\bar{N}$ is an integer equal to 4, 5, 10, or 11.

The fugacity of water in the empty hydrate lattice, f_w^β in eq A.25, is given by[101]

$$f_w^\beta = f_w^{I/L} \exp\left(\frac{\Delta\mu_w^{\beta-I/L}}{RT}\right) \tag{A.31}$$

where $f_w^{I/L}$ is the fugacity of pure ice or liquid water, and the quantity inside the parentheses is given by the following equation[101,104]

$$\frac{\Delta\mu_w^{\beta-I/L}}{RT} = \frac{\mu_w^\beta(T,P)}{RT} - \frac{\mu_w^{I/L}(T,P)}{RT}$$

$$= \frac{\Delta\mu_w^0}{RT_0} - \int_{T_0}^{T}\frac{\Delta h_w^{\beta-I/L}}{RT^2}dT + \int_0^P \frac{\Delta v_w^{\beta-I/L}}{RT}dP \tag{A.32}$$

where μ_w^β and $\mu_w^{I/L}$ are the chemical potential of the empty hydrate lattice and of pure water in the ice (I) or the liquid (L) state, respectively. $\Delta\mu_w^0$ is the reference chemical potential difference between water in the empty hydrate lattice and pure water in the ice phase at 273.15 K. $\Delta h_w^{\beta-I/L}$ and $\Delta v_w^{\beta-I/L}$ are the molar enthalpy and molar volume differences between an empty hydrate lattice and ice or liquid water. $\Delta h_w^{\beta-I/L}$ is given by the following equation[101,104]

$$\Delta h_w^{\beta-I/L} = \Delta h_w^0 + \int_{T_0}^{T}\Delta C_{pw}dT \tag{A.33}$$

where Δh_w^0 is the enthalpy difference between the empty hydrate lattice and ice, at the ice point and zero pressure. The heat capacity difference between the empty hydrate lattice and the pure liquid water phase, ΔC_{pw}, is also temperature dependent, and the equation recommended by Holder et al.[104] is used

$$\Delta C_{pw} = -37.32 + 0.179(T - T_0)\ T > T_0 \tag{A.34}$$

where ΔC_{pw} is in $J\ mol^{-1}\ K^{-1}$. Furthermore, the heat capacity difference between hydrate structures and ice is set equal to zero. The reference properties used are summarized in Table 6.

Calculation of Fugacity Coefficient Using an *EoS*. The following general form can be used for expressing any cubic equation of state:[111]

$$P = \frac{RT}{v - b} - \frac{a}{v^2 + uv - w^2} \tag{A.35}$$

The fugacity coefficient for component i in a mixture can be expressed as[111]

$$\ln\phi_i = -\ln(Z - B) + \frac{B_i' B}{Z - B} + \frac{A}{\sqrt{U^2 + 4W^2}}\left[A_i' - \frac{U_i'U^2 + 4W_i'W^2}{U^2 + 4W^2}\right] \times \ln\left[\frac{2Z + U - \sqrt{U^2 + 4W^2}}{2Z + U + \sqrt{U^2 + 4W^2}}\right] - A\left[\frac{2(2Z + U)W_i'W^2 + (UZ - 2W^2)U_i'U}{(Z^2 + UZ - W^2)(U^2 + 4W^2)}\right] \tag{A.36}$$

where

$$A = \frac{Pa}{(RT)^2}, \qquad B = \frac{Pb}{RT} \tag{A.37,A.38}$$

$$U = \frac{Pu}{RT}, \qquad W = \frac{Pw}{RT} \tag{A.39,A.40}$$

$$Z = \frac{Pv}{RT} \tag{A.41}$$

and

$$A_i' = \frac{1}{na}\left[\frac{\partial(n^2a)}{\partial n_i}\right]_{T,n_{j\neq i}}, \quad B_i' = \frac{1}{b}\left[\frac{\partial(nb)}{\partial n_i}\right]_{T,n_{j\neq i}} \tag{A.42,A.43}$$

$$U_i' = \frac{1}{u}\left[\frac{\partial(nu)}{\partial n_i}\right]_{T,n_{j\neq i}}, \quad W_i' = \frac{1}{w}\left[\frac{\partial(nw)}{\partial n_i}\right]_{T,n_{j\neq i}} \tag{A.44,A.45}$$

The compressibility factor Z is given by the following dimensionless equation:[111]

$$Z^3\text{-}(1+B-U)Z^2+(A\text{-}BU-U-W^2)Z\text{-}(AB-BW^2\text{-}W^2) = 0 \tag{A.46}$$

Nomenclature

AD = absolute deviation
BIP = binary interaction parameter
EoS = equation of state
FID = flame ionization detector
GC = gas chromatography
HC = hydrocarbon
MW = microwave
NDD = nondensity dependent mixing rules
NIR = near-infrared
PID = proportional integrator derivative controller
PR = Peng−Robinson equation of state
TCD = thermal conductivity detector
TDLAS = tunable diode laser absorption spectroscopy
Vol = volume of the loop
VPT−EoS = Valderrama modification of Patel-Teja equation of state
C = Langmuir constant
F = parameter of the equation of state
G = gas
H = hydrate
I = ice
L = liquid
M = metal of valence x
N = number of experimental points
$\bar{N}$ = an integer equal to 4, 5, 10, or 11
P = pressure

Q = quadruple point
R = universal gas constant
$\bar{R}$ = cavity radius
T = temperature
V = vapor
$\bar{V}$ = volume
Z = compressibility factor
nc = number of components
ppb = part per billion
ppm = part per million
ppt = part per trillion
sI = structure-I
sII = structure-II
sH = structure-H
a = attractive parameter of the equation of state
$\bar{a}$ = parameter of the equation of state
b = parameter of the equation of state
c = parameter of the equation of state
f = fugacity
g = gas
k = binary interaction parameter for the classical mixing rules
k' = Boltzmann's constant
l = binary interaction parameter for the asymmetric term
n = number of moles
r = distance
u = parameter of the equation of state in general form
v = molar volume
$\bar{v}$ = number of cavities of type m per water molecule in the unit cell
w = parameter of the equation of state in general form
$w(r)$ = spherically symmetric cell potential function
x = liquid mol fraction
y = vapor mol fraction
z = coordination number

Greek Letters

ΔC_{pw} = heat capacity difference between the empty hydrate lattice and liquid water
ΔC_{pw}° = reference heat capacity difference between the empty hydrate lattice and liquid water at 273.15 K
Δh_w = enthalpy difference between the empty hydrate lattice and ice/liquid water
Δh_w° = enthalpy difference between the empty hydrate lattice and ice at ice point and zero pressure
Δv_w = molar volume difference between the empty hydrate lattice and ice/liquid water
$\Delta \mu_w$ = chemical potential difference between the empty hydrate lattice and ice/liquid water
$\Delta \mu_w^{\circ}$ = chemical potential difference between the empty hydrate lattice and ice at ice point and zero pressure
$\Delta \mu_w^{\beta-H}$ = chemical potential difference of water between the empty hydrate lattice and the hydrate phase
$\Delta \mu_w^{\beta-I/L}$ = chemical potential difference of water between the empty hydrate lattice and the ice/liquid water phase
Ψ = power parameter in the $VPT-EoS$
Ω = parameter in the $VPT-EoS$
α = Kihara hard-core radius
$\alpha(T_r)$ = temperature-dependent function
ϵ = characteristic energy
ϕ = fugacity coefficient
γ = activity coefficient
μ = chemical potential
σ = collision diameter
$\sigma^* = \sigma - 2\alpha$
ω = acentric factor
Γ = potential energy of interaction between two molecules

Superscripts

A = asymmetric properties
C = classical properties
H = hydrate
I = ice
L = liquid
T = total
V = vapor
$loop$ = loop
ref = reference property
sat = property at saturation
β = empty hydrate lattice
∞ = infinite dilution
0 = reference property
1 = nontemperature-dependent term in NDD mixing rules
2 = temperature-dependent term in NDD mixing rules

Subscripts

HC = hydrocarbon compound
I = ice
T = total
$dilutor$ = dilutor
exp = experimental property
min = minimum
max = maximum
prd = predicted property
a = index for properties
b = index for properties
c = critical property
c_* = index for properties
i, j = molecular species
m = type m of cavities
p = polar compound
r = reduced properties
w = water
x = valence
0 = reference property
1 = first quadruple point
2 = second quadruple point

Literature Cited

(1) Bukacek, R. F. *Institute of Gas Technology* 1955, Research Bulletin 8.

(2) Sharma, S.; Campbell, J. M. *Oil Gas J*. **1969**, *67(31)*, 136−137 (quoted in refs 110 and 112).

(3) Robinson, J. N.; Moore, R. G.; Heidemann, R. A.; Wichert, E. *Oil Gas J*. **1978**, *76(5)*, 76−78 (quoted in ref 110).

(4) Maddox, R. N.; Lilly, L. L.; Moshfeghian, M.; Elizondo, E. *Laurance Reid Gas Conditioning Conference*, March 1988, Norman, OK (quoted in ref 110).

(5) Wichert, G. C.; Wichert, E. *Oil Gas J*. **1993**, *90(13)*, 61−64 (quoted in ref 110).

(6) Gas Processors Suppliers Association and Gas Processors Association. *GPSA Engineering Data Book*, 11th ed.; Tulsa, OK, 1999 (quoted in ref 110).

(7) Ning, Y.; Zhang, H.; Zhou, G. *Chem. Eng. Oil Gas* **2000**, *29*, 75−77 (in Chinese, quoted in ref 110).

(8) Valderrama, J. O. *J. Chem. Eng. Jpn.* **1990**, *23*, 87−91.

(9) Avlonitis, D.; Danesh, A.; Todd, A. C. *Fluid Phase Equilibria* **1994**, *94*, 181−216.

(10) van der Waals, J. H.; Platteeuw, J. C. *Adv. Chem. Phys.* **1959**, *2*, 1−57.

(11) Gas Quality. Proceeding of the congress, Specification and measurement of physical and chemical properties of natural gas; van Rossum, G. J., Ed.; Groningen, The Netherlands, April 22−25, 1986, Amsterdam: Elsevier Science Publishers B.V.

(12) Duswalt, A.; Brandt, W. *Anal. Chem.* **1960**, *32*, 272−274.

(13) Sundberg, O. E.; Maresh, C. *Anal. Chem.* **1960**, *32*, 274−277.

(14) Knight, H. S.; Weiss, F. T. *Anal. Chem.* **1962**, *34*, 749−751.

(15) Goldup, A.; Westaway, M. T. *Anal. Chem.* **1966**, *38*, 1657−1661.

(16) Kaiser, R. *Chromatographia* **1969**, *2*, 453−461.

(17) Neumann, G. M. *Z. Anal. Chem.* **1969**, *244*, 302−305.

(18) Latif, S.; Haken, J. K. *J. Chromatogr.* **1983**, *258*, 233−237.

(19) Tianhui, D.; Baoq, L.; Hongyi, Z.; Yanfang, L. *Analyst* **1992**, *117*, 1577−1579.
(20) Yajima, S.; Shiba, K.; Handa, M.; Takahashi, Y. *Bull. Chem. Soc. Jpn.* **1974**, *37*, 800−804.
(21) Kong, V. C. Y.; Foukles, F. R.; Kirk, D. W.; Hinatsu, J. T. *Int. J. Hydrogen Energy* **1999**, *24*, 665−675.
(22) Chapoy, A.; Coquelet, C.; Richon, D. *Fluid Phase Equilibria* **2003**, *214*, 101−117.
(23) Dhima, A.; Noll, O.; Valtz, A.; Richon, D. *18th European Seminar on Applied Thermodynamics*, June 8−11th, 2000, Kutna Hora, Czech Republic.
(24) Althaus, K. *Fortschritt − Berichte VDI* 1999, Reihe 3, 350 (in German). Oellrich, L. R.; Althaus, K. GERG − Water Correlation (GERG Technical Monograph TM14) Relationship Between Water Content and Water Dew Point Keeping in Consideration the Gas Composition in the Field of Natural Gas. *Fortschritt − Berichte VDI* 2000, Reihe 3- Nr. 679 (in English).
(25) Ugrozov, V. V. *Zh. Fiz. Khim.* **1996**, *70*, 1328−1329 (in Russian).
(26) Yokoyama, C.; Wakana, S.; Kaminishi, G. I.; Takahashi, S. *J. Chem. Eng. Data* **1988**, *33*, 274−276.
(27) Yarym-Agaev, N. L.; Sinyavskaya, R. P.; Koliushko, I. I.; Levinton, L. Ya. *Zh. Prikladnoi Khim.* **1985**, *58(1)*, 165−168 (in Russian).
(28) Gillespie, P. C.; Wilson, G. M. GPA, Tulsa, OK, Research Report 48, 1982.
(29) Kosyakov, N. E.; Ivchenko, B. I.; Krishtopa, P. P. *Vopr Khim. Tekhnol.* **1982**, *47*, 33−36.
(30) Aoyagi, K.; Song, K. Y.; Kobayashi, R.; Sloan, E. D.; Dharmawardhana, P. B. GPA, Tulsa, Research Report 45, 1980.
(31) Kosyakov, N. E.; Ivchenko, B. I.; Krishtopa, P. P. *Zh. Prikladnoi Khim.* **1979**, *52(4)*, 922−923.
(32) Aoyagi, K.; Song, K. Y.; Sloan, E. D.; Dharmawardhana, P. B.; Kobayashi, R. *58th Annual GPA Convention*, March 19−21, 1979, Denver, Colorado.
(33) Sloan, E. D.; Khoury, F. M.; Kobayashi, R. *Ind. Eng. Chem. Fundam.* **1976**, *15(4)*, 318−322.
(34) Sharma, S. C. Ph.D. Thesis, University of Oklahoma, Norman, 1969 (quoted in Robinson, J. N.; Moore, R. G.; Heideman, R. A.; Wichert, E. *SPE J.* **1977**, 281−286).
(35) Rigby, M.; Prausnitz, J. M. *J. Phys. Chem.* **1968**, *72(1)*, 330−334.
(36) Lukacs, J.; Robinson, D. B. *SPE J.* **1963**, 293−297.
(37) Olds, R. H.; Sage, B. H.; Lacey, W. N. *Ind. Eng. Chem.* **1942**, *34(10)*, 1223−1227.
(38) Chapoy, A.; Coquelet, C.; Richon, D. *J. Chem. Eng. Data* **2003**, *48*, 957−966.
(39) Song, K. Y.; Kobayashi, R. *Fluid Phase Equilibria* **1994**, *95*, 281−298.
(40) Namiot, A. Yu. Rastvorimost' gazov v vode. Spravochnoe posobie, Moscow: Nedra, 1991 (quoted in ref 25).
(41) Song, K. Y.; Kobayashi, R. GPA, Tulsa, OK, Research Report 132, 1991.
(42) Sloan, E. D.; Sparks, K. A.; Johnson, J. J. *Ind. Eng. Chem. Res.* **1987**, *26*, 1173−1179.
(43) Bourrie, M. S.; Sloan, E. D. GPA, Tulsa, OK, Research Report 100, June 1986.
(44) Sparks, K. A.; Sloan, E. D. GPA, Tulsa, Research Report 71, September 1983.
(45) Parrish, W. R.; Pollin, A. G.; Schmidt, T. W. *Proc. 61st Ann. Conv. Gas Process. Assoc.* 1982, Dallas, TX.
(46) Pollin et al. Internal Report, Phillips Petroleum Co., 1982 (quoted in ref 44).
(47) Coan, C. R.; King, A. D. *J. Am. Chem. Soc.* **1971**, *93*, 1857−1862.
(48) Anthony, R. G.; McKetta, J. J. *J. Chem. Eng. Data* **1967**, *12(1)*, 17−20.
(49) Anthony, R. G.; McKetta, J. J. *J. Chem. Eng. Data* **1967**, *12(1)*, 21−28.
(50) Reamer, H. H.; Olds, R. H.; Sage, B. H.; Lacey, W. N. *Ind. Eng. Chem.* **1943**, *35*, 790−793.
(51) Kahre, L. C. Internal Report, Phillips Petroleum Co. 1964 (Also, Kahre, L. C. Internal Report, Phillips Petroleum Co. 1968, Bartlesville, OK).
(52) Kobayashi, R.; Katz, D. L. *Ind. Eng. Chem* **1953**, *45(2)*, 440−451.
(53) Kobayashi, R. Ph.D. Thesis, University of Michigan, 1951.
(54) Poettmann, F. H.; Dean, M. R. *Pet. Refiner* **1946**, *25(12)*, 125−128.
(55) Chaddock, R. E. Ph.D. Dissertation, University of Michigan, 1940.
(56) Perry, C. W. *Ind. Eng. Chem. Anal. Ed.* **1938**, *10(9)*, 513−514.
(57) Hachmuth, K. H. *Western Gas* **1931**, *8(1)*, 55.
(58) McKetta, J. J. and co-workers, unpublished data (quoted in Hoot, W. F.; Azarnoosh, A.; McKetta, J. J. *Pet. Refiner* **1957**, *36(5)*, 255−256).
(59) McKetta, J. J. private communications.
(60) Wehe, A. H.; McKetta, J. J. *J. Chem. Eng. Data* **1961**, *6(2)*, 167−172.
(61) Reamer, H. H.; Sage, B. H.; Lacey, W. N. *Ind. Eng. Chem.* **1952**, *44*, 609−615 (Also, Reamer, H. H.; Sage, B. H.; Lacey, W. N. American Documentation Institute, Washington, DC, 1950, Doc. No. 3328).
(62) Brooks, W. B.; Gibbs, G. B.; McKetta, J. J. *Pet. Refiner* **1951**, *30(10)*, 118−120.
(63) Black, C.; Joris, G. G.; Taylor, H. S. *J. Chem. Phys.* **1948**, *16*, 537.
(64) McKetta, J. J.; Katz, D. L. *Trans. AIME, Petrol. Div.* **1947**, *170*, 34−43.
(65) Reamer, H. H.; Olds, R. H.; Sage, B. H.; Lacey, W. N. *Ind. Eng. Chem.* **1944**, *36*, 381−383.
(66) Dohrn, R.; Bünz, A. P.; Devlieghere, F.; Thelen, D. *Fluid Phase Equilibria* **1993**, *83*, 149−158.
(67) King, M. B.; Mubarak, A.; Kim, J. D.; Bott, T. R. *J. Supercritical Fluids* **1992**, *5*, 296−302.
(68) D'Souza, R.; Patrick, J. R.; Teja, A. S. *Can. J. Chem. Eng.* **1988**, *66*, 319−323.
(69) Müller, G.; Bender, E.; Maurer, G. *Ber. Bunsen-Ges. Phys. Chem.* **1988**, *92*, 148−160.
(70) Briones,J. A.; Mullins, J. C.; Thies, M. C.; Kim, B.-U. *Fluid Phase Equilibria* **1987**, *36*, 235−246.
(71) Nakayama, T.; Sagara, H.; Arai, K.; Saito, S. *Fluid Phase Equilibria* **1987**, *38*, 109−127.
(72) Song, K. Y.; Kobayashi, R. *SPE Formation Evaluation* 1987, 500−508.
(73) Song, K. Y.; Kobayashi, R. GPA, Tulsa, OK, Research Report 99, June 1986.
(74) Song, K. Y.; Kobayashi, R.; Marsh, W. GPA, Research Report 80, Tulsa, OK, May 1984.
(75) Gillespie, P. C.; Owens, J. L.; Wilson, G. M. *AIChE Winter National Meeting*, March 11−14, 1984, Paper 34-b, Atlanta, GA.
(76) Chrastil, J. *J. Phys. Chem.* **1982**, *86*, 3016−3021.
(77) Zawisza, A.; Malesinska, B. *J. Chem. Eng. Data* **1981**, *26(4)*, 388−391.
(78) Kobayashi, R.; Aoyagi, K.; Takahashi, S.; Song, K. Y. *Final Revised Report on the Water Content of Carbon Dioxide Gas and Liquid in Equilibrium with Liquid Water and with Gas Hydrates Reported to ARCO Oil and Gas Company*, June 1979, Dallas, TX.
(79) Takenouchi, S.; Kennedy, G. C. *Am. J. Sci.* **1964**, *262*, 1055−1074.
(80) Tödheide, K.; Franck, E. U. *Z. Phys. Chem.* (Frankfurt am Main) **1963**, 387−401 (quoted in Robinson, J. N.; Moore, R. G.; Heideman, R. A.; Wichert, E. *SPE J.* August **1977**, 281−286).
(81) Malinin, S. D. *GeoChem.* **1959**, *No. 3*, 292−306.
(82) Sidorov, I. P.; Kazarnovsky, Y. S.; Goldman, A. M. *Tr. Gosudarst. Nauch.-Issled. I Proekt. Inst. Azot. Prom.* **1953**, *1*, 48 (data from Dortmund Data Base).
(83) Stone, H. W. *Ind. Eng. Chem.* **1943**, *35(12)*, 1284−1286.
(84) Wiebe, R.; Gaddy, V. L. *J. Am. Chem. Soc.* **1941**, *63*, 475−477 (quoted in Wiebe, R. *Chem. Rev.* **1941**, *29*, 475−481).
(85) Pollitzer, F.; Strebel, E. *Z. Phys. Chem.* **1924**, *110*, 768−785.
(86) Gillespie, P. C.; Wilson, G. M. GPA, Tulsa, OK, Research Report 41, April 1980.
(87) Kosyakov, N. E.; Ivchenko, B. I.; Krishtopa, P. P. *Zh. Prikladnoi Khim.* **1977**, *50(11)*, 2568−2570 (in Russian).
(88) Maslennikova, V. Ya.; Vdovina, N. A.; Tsiklis, D. S. *Zh. Fiz. Khim.* **1971**, *45(9)*, 1354 (in Russian).
(89) Namiot, A. Yu.; Bondareva, M. M. Rastvorimost' gazov v vode, Moscow: Gostekhizdat, 1959 (quoted in ref 25).
(90) Saddington, A. W.; Krase, N. W. *J. Am. Chem. Soc.* **1934**, *56*, 353−361 (quoted in ref 1).
(91) Bartlett, E. P. *J. Am. Chem. Soc.* **1927**, *49*, 65−78 (quoted in ref 1).
(92) Gillespie, P. C.; Wilson, G. M. GPA, Tulsa, OK, Research Report 48, April 1982.

(93) Lee, J.; Mather, A. E. *Berichte der Bunsen − Gesellschaft* **1977**, *81(10)*, 1020−1023.

(94) Selleck, F. T.; Carmichael, L. T.; Sage, B. H. *Ind. Eng. Chem.* **1952**, *44(9)*, 2219−2226 (Also, Selleck, F. T.; Carmichael, L. T.; Sage, B. H. American Documentation Institute, Washington, DC, 1951, Doc. No. 3570).

(95) Wright, R. H.; Maass, O. *Can. J. Res.* **1932**, *6*, 94−101.

(96) Guilbot, P.; Valtz, A.; Legendre, H.; Richon, D. *Analusis* **2000**, *28*, 426−431.

(97) Avlonitis, D. A. MSc. Thesis, Heriot-Watt University, 1988.

(98) Avlonitis, D. A. Ph.D. Thesis, Heriot-Watt University, 1992.

(99) Tohidi, B.; Burgass, R. W.; Danesh, A.; Todd, A. C. *SPE 26701, Proceedings of the SPE Offshore Europe 93 Conference* 1993, 255−264.

(100) Tohidi-Kalorazi, B. Ph.D. Thesis, Heriot-Watt University, 1995.

(101) Anderson, F. E.; Prausnitz, J. M. *AIChE J.* **1986**, *32*(8), 1321−1332.

(102) Parrish, W. R.; Prausnitz, J. M. *Ind. Eng. Chem. Proc. Des. Dev.* **1972**, *11*, 26−35.

(103) McKoy, V.; Sinanoglu, O. *J. Chem. Phys.* **1963**, *38(12)*, 2946−2956 (quoted in ref 102).

(104) Holder, G. D.; Corbin, G.; Papadopoulos, K. D. *Ind. Eng. Chem. Fundam.* **1980**, *19*, 282−286.

(105) Dharmawardhana,P. B.; Parrish, W. R.; Sloan, E. D. *Ind. Eng. Chem. Fundam.* **1980**, *19*, 410−414.

(106) Sloan, E. D. Second Edition, Marcel Dekker: New York, 1998.

(107) Anderko, A. *Fluid Phase Equilibria* **1990**, *61*, 145−225.

(108) Chapoy, A.; Mohammadi, A. H.; Richon, D.; Tohidi, B. *Fluid Phase Equilibria* **2004**, *220*, 113−121.

(109) Carroll, J. J. Gulf Professional Publishing: 2003 (Also, Carroll, J. J. *The 81st Annual GPA Convention* March 11−13, 2002, Dallas, Texas).

(110) Daubert, T. E.; Danner, R. P. AIChE: New York, 1985 (quoted in ref 114).

(111) Danesh, A. first ed.; Elsevier: Amsterdam, 1998.

Received for review February 26, 2004
Revised manuscript received July 23, 2004
Accepted August 11, 2004

IE049843F